

Resonance Raman spectroscopy of G-line and folded phonons in twisted bilayer graphene with large rotation angles

Yanan Wang, Zihua Su, Wei Wu, Shu Nie, Nan Xie, Huiqi Gong, Yang Guo, Joon Hwan Lee, Sirui Xing, Xiaoxiang Lu, Haiyan Wang, Xinghua Lu, Kevin McCarty, Shin-shem Pei, Francisco Robles-Hernandez, Viktor G. Hadjiev, and Jiming Bao

Citation: [Applied Physics Letters](#) **103**, 123101 (2013); doi: 10.1063/1.4821434

View online: <http://dx.doi.org/10.1063/1.4821434>

View Table of Contents: <http://scitation.aip.org/content/aip/journal/apl/103/12?ver=pdfcov>

Published by the [AIP Publishing](#)

Advertisement:

The advertisement features a photograph of various optical components like mirrors, beam splitters, and prisms on the left. The right side contains text describing the PulseLine product family and listing specific products available.

PulseLine™ Ultrafast Laser Optics

The PulseLine family includes a number of standard, in-stock products which are ready to ship, and fully customized optics for volume applications

PULSELINE PRODUCTS

- MIRRORS
- BEAMSPLITTERS
- POLARIZING OPTICS (PLATES AND CUBES)
- PRISMS
- ANTI-REFLECTION WINDOWS

CVI Laser Optics
cvilaseroptics@idexcorp.com
cvilaseroptics.com

IDEX
OPTICS & PHOTONICS

ATFilms | Precision Photonics | CVI Laser Optics | Melles Griot | Semrock

Resonance Raman spectroscopy of G-line and folded phonons in twisted bilayer graphene with large rotation angles

Yanan Wang,¹ Zhihua Su,¹ Wei Wu,^{1,2} Shu Nie,³ Nan Xie,⁴ Huiqi Gong,⁴ Yang Guo,⁴ Joon Hwan Lee,⁵ Sirui Xing,^{1,2} Xiaoxiang Lu,¹ Haiyan Wang,⁵ Xinghua Lu,⁴ Kevin McCarty,³ Shin-shem Pei,^{1,2} Francisco Robles-Hernandez,⁶ Viktor G. Hadjiev,⁷ and Jiming Bao^{1,a)}

¹Department of Electrical and Computer Engineering University of Houston, Houston, Texas 77204, USA

²Center for Advanced Materials, University of Houston, Houston, Texas 77204, USA

³Sandia National Laboratories, Livermore, California 94550, USA

⁴Institute of Physics, Chinese Academy of Sciences, Beijing 100190, China

⁵Department of Electrical and Computer Engineering, Texas A&M University, College Station, Texas 77843, USA

⁶College of Engineering Technology, University of Houston, Houston, Texas 77204, USA

⁷Texas Center for Superconductivity and Department of Mechanical Engineering, University of Houston, Houston, Texas 77204, USA

(Received 24 July 2013; accepted 26 August 2013; published online 16 September 2013)

We report the synthesis and systematic Raman study of twisted bilayer graphene (tBLG) with rotation angles from below 10° to nearly 30° . Chemical vapor deposition was used to grow hexagon-shaped tBLG with a rotation angle that can be conveniently determined by relative edge misalignment. Rotation dependent G-line resonances and folded phonons were observed by selecting suitable energies of excitation lasers. The observed phonon frequencies of the tBLG superlattices agree well with our *ab initio* calculation. © 2013 AIP Publishing LLC.
<http://dx.doi.org/10.1063/1.4821434>

Twisted bilayer graphene (tBLG) has attracted considerable attention recently because of the tunability of interlayer coupling and band structure resulting from the freedom of relative rotation.^{1–15} The unique properties of tBLG have been revealed by Raman spectroscopy,^{10–15} and they provide an enormous opportunity for device applications. However, tBLG samples used in these reported experimental studies are not well suitable for device applications.^{5–7,10–13,15} One problem is that rotation angles of tBLG cannot be conveniently determined. Sophisticated techniques such as transmission electron microscopy (TEM), scanning tunneling microscopy (STM), and atomic force microscopy (AFM) were often used. Another problem is that bilayer regions of interest are not well isolated from the rest of graphene. Because of the lack of suitable tBLG samples, especially with rotation angles greater than 16° , a well-characterized G-line resonances is still missing, and a one-to-one relationship between G-line resonance, folded phonon frequency, and rotation angle has not been established.^{6,10–13,15}

Twisted bilayer graphene was grown on Cu foils by chemical vapor deposition (CVD) at ambient pressure in a quartz tube furnace.¹⁶ The conditions are similar to what we used for single-layer graphene,^{17,18} except that a larger flow rate of CH_4 was used to facilitate the growth of bilayer graphene.¹⁹ Figures 1(a)–1(d) show examples of bilayer graphene islands that consist of two graphene hexagons stacked on each other. It can be seen that two layers can have relative rotation angles from 0° to nearly 30° . The lattice rotation is confirmed by investigations of TEM and STM.¹⁹ The effect of lattice rotation on the electronic band structure is also revealed by the STM observation of Van Hove singularities.^{19,20} An important advantage of such bilayer graphene

structures compared to those previously reported is that the relative edge misorientation of two hexagons represents their actual lattice rotation. This conclusion is obtained by comparing low-energy electron diffraction (LEED) with low-energy electron microscopy (LEEM) from the same region of graphene.¹⁶ The relationship between edge misorientation and lattice rotation has facilitated the identification of tBLG, where rotation angles in this work are all based on the average edge misorientations. Similar stacked graphene hexagons were reported before, but their lattice rotation was not verified

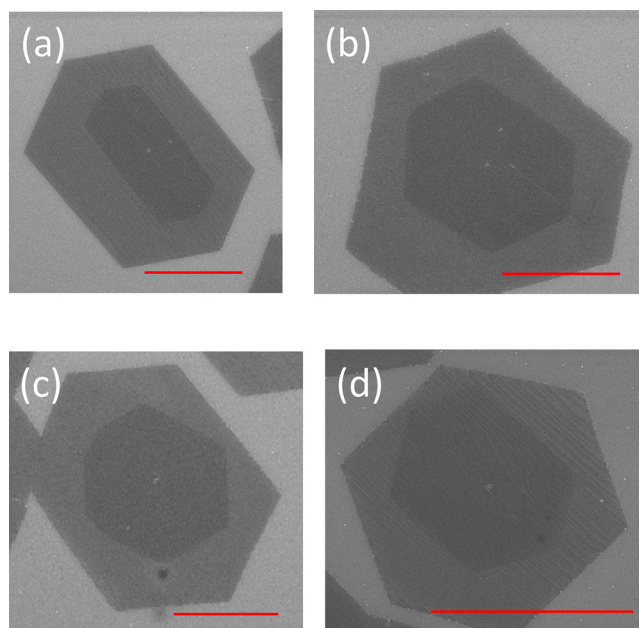


FIG. 1. Scanning electron microscopy (SEM) pictures of representative tBLG hexagons with various rotation angles. Scale bars: 5 μm .

^{a)}jbao@uh.edu

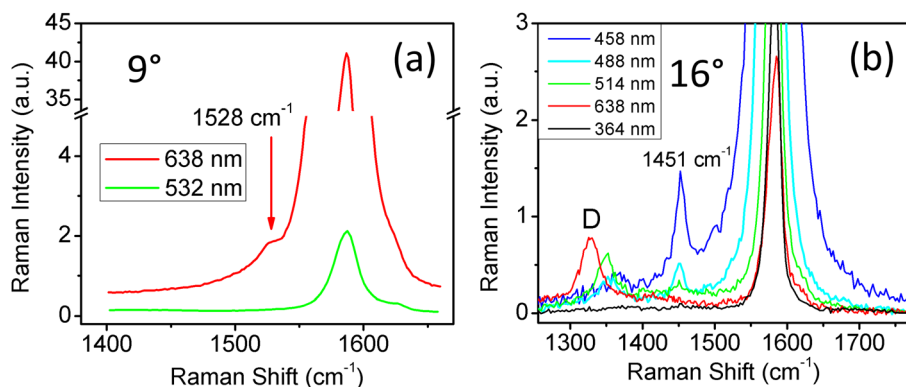


FIG. 2. Raman spectra of G-line and folded TO phonons under different laser excitation energies in two tBLG with rotation angles of 9° (a) and 16° (b). The spectra are normalized relative to the G-line of single-layer graphene.

with direct lattice imaging techniques such as TEM, STM, or LEED.²¹

Resonance Raman scatterings of G-line and folded phonon can be conveniently observed in tBLG samples with rotation angles around 12° because the resonance excitation energy falls in the range of our five visible laser lines from 638 nm to 458 nm. Figure 2 shows representative Raman spectra of two tBLG with 9° and 16° rotation angles. As can be seen, the intensities of folded phonons follow the same dependence on laser excitation wavelength as G-line. For the 9° tBLG, the G-line resonance was only observed with the 638-nm laser. The resonance was centered around 458-nm for 16° tBLG, and it disappeared when the laser was switched to either 638-nm or 364-nm. The dependence of folded phonon frequency on the rotation angle can also be clearly seen: The frequency decreases when the rotation angle increases.

According to previous calculations, G-line resonance should be observed even for tBLG with a large rotation angle if the excitation energy is tuned high enough.^{10,13} This prediction is verified when a 364-nm UV laser was used. Figure 3 shows a more than 30 times enhancement in G-line intensity when a tBLG 25.6° sample was excited by the UV line. It should be noted that UV lasers were used in the observation of phonons in twisted bilayer graphene,^{15,22} but a direct G-line enhancement compared to that of single layer graphene was not reported, and the rotation angle was not provided. But where is the folded phonon? We show that the

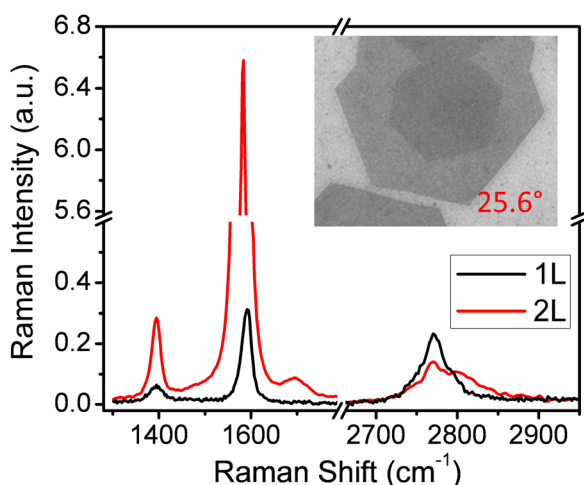


FIG. 3. 364-nm UV Raman spectra from single-layer (1L) and bilayer (2L) regions of a $\sim 25.6^\circ$ tBLG. Inset: SEM image.

strong Raman peak near D-line position is actually the folded phonon.

This assignment of the folded phonon is based on the following observations. First, the position of this peak is dependent on the rotation angle of tBLG. Figures 4(a)–4(c) show a series of UV Raman spectra in six different samples including the 16° tBLG. It can be seen that the peak positions of 2D-band remain almost the same, but a large shift in the positions of Raman peaks near the D-line is observed. According to the relationship between D-line and 2D-band, the Raman shift of the D-line is simply half the Raman shift of the 2D-band. Thus, the strong Raman near D-line cannot be the usual D-line as observed by visible laser lines. Second, as before, such strong Raman peaks near D-line are only observed when there is G-line resonance. This is supported by all six samples shown in Figs. 3(a)–3(c). Because the 16° sample exhibits no G-line enhancement, there is no observable peak near the usual D-line. The other five samples show different degrees of G enhancement from 5 to 20 times. Unlike Raman with visible laser lines, the UV Raman D-line is very weak: the relatively strong D-line in single-layer graphene shown in Fig. 3 is due to the defects created by UV exposure during the Raman.²³ The dependence of observed phonon frequencies on the rotation angle is summarized in Fig. 4(d). A general trend can be observed: A larger rotation angle leads to a lower phonon frequency.

Folded phonons are frequently observed in 1-D superlattices.^{24,25} The frequency of folded phonons can be estimated by zone folding of the initial phonon dispersion curve into the reduced Brillouin zone (rBZ) of the superlattices. Conversely, the character of folded phonon is an important measure of the quality of superlattice structure.²⁴ Figure 4(a) shows BZ of single-layer graphene and rBZ of the bilayer superlattice with a rotation angle of 13.2° . Also shown are two sets of six-fold reciprocal lattices A and B of the superlattice. It is the position of these reciprocal lattices that determine the frequency of folded phonons. This can be understood in the following two ways using reciprocal lattice A as an example. When transverse optical (TO) dispersion in the larger BZ of single-layer graphene (SLG) is mapped into the reduced BZ of the superlattice, point A will be mapped to the Γ -point of the BZ, and becomes Γ -point optical phonons that can be probed by Raman scattering. Based on the six-fold symmetry, phonons at six reciprocal lattices equivalent to lattice A will have the same frequency. Its frequency can be calculated directly for the specific point A in the SLG BZ.^{9,11,19} For this purpose, we

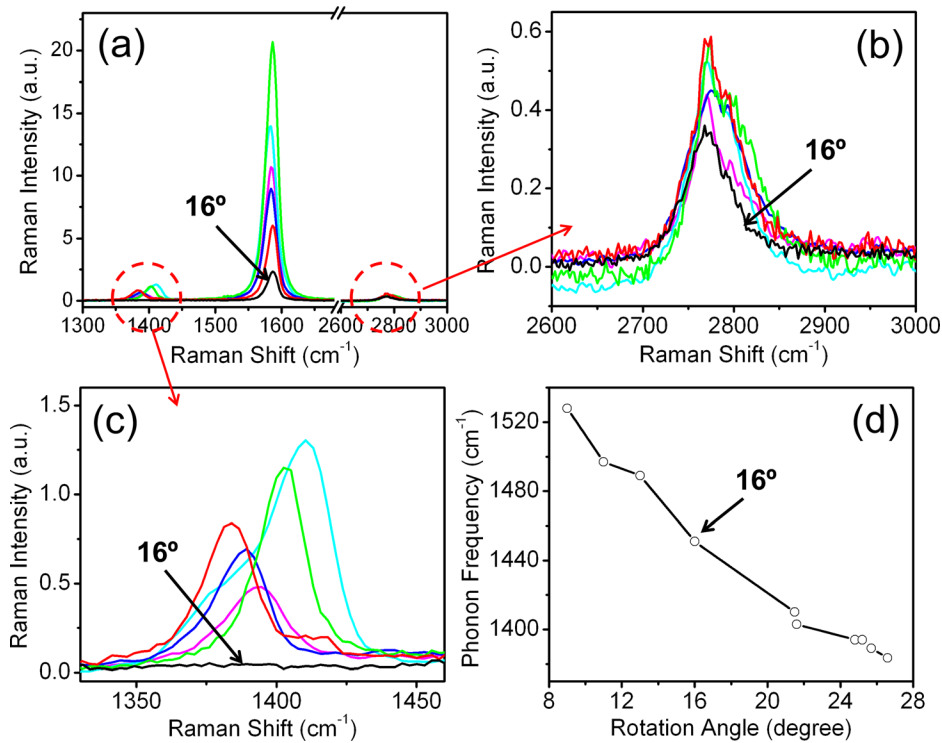


FIG. 4. (a)–(c): 364-nm UV Raman spectra of the 16° (black) tBLG and five other tBLGs with rotation angles greater than 21 degrees. (a): Raman spectra indicating G-line resonance with an enhancement of 5 to 20 times for large-angle tBLGs. There is no G-line resonance for the 16-degree tBLG. (b): Close-up view of (a) near 2D-band. (c): Close-up view of (a) near 1400 cm⁻¹. (d): Observed phonon frequency as a function of rotation angle.

note that the rBZ in Figure 5(a) nearly coincides with that of the Moiré reciprocal lattice of tBLG at the same angle. The Moiré lattice BZ vector $q(\theta) = \frac{8\pi}{\sqrt{3}a} \sin(\frac{\theta}{2})$ then is equal to Γ -A momentum.^{11,14} Figure 5(b) compares the experimental folded phonon frequencies (open circles) with those calculated¹⁹ for point A in SLG BZ (red curve) at angles θ between 0° and 30°. Both sets of frequencies are plotted against the Moiré vector $q(\theta)$. The experimental frequencies follow closely the calculated frequency dependence, which suggests that the Moiré lattice is a good approximation to the tBLG superlattice realized in our samples.

According to the zone folding shown in Fig. 5(a), two different phonon modes are expected from reciprocal lattices A and B, but a lower-frequency phonon at B has not been observed. This is the case for all of the samples we have measured. We believe the following reasons explain why only the phonon with the highest frequency is observed. Let us take the 13.2° tBLG as an example. First, the crystal momentum Γ -A is the fundamental reciprocal lattice vector of the superlattice, while Γ -B represents a higher-order crystal momentum. Raman scattering is typically much stronger for processes involving the fundamental mode than the higher order modes. Second, the phonon Γ -A is closer in energy to the G-line compared with the folded phonon Γ -B. The Γ -A phonon is thus more likely to be resonantly excited when the resonance condition for the G-line is satisfied.^{9,11}

It was speculated by the continuum model that the inter-layer coupling becomes negligible for a tBLG with a large rotation angle.¹ But our observations indicate that this is not the case: A G-line resonance and a relatively strong folded phonon are observed for large-angle twisted graphene. This observation agrees with the calculation based on a graphene superlattice, and it is a result of a smaller size of unit cell of the superlattice for larger rotation angles.⁸ The fact that both G-line resonance and folded phonons are observed for any

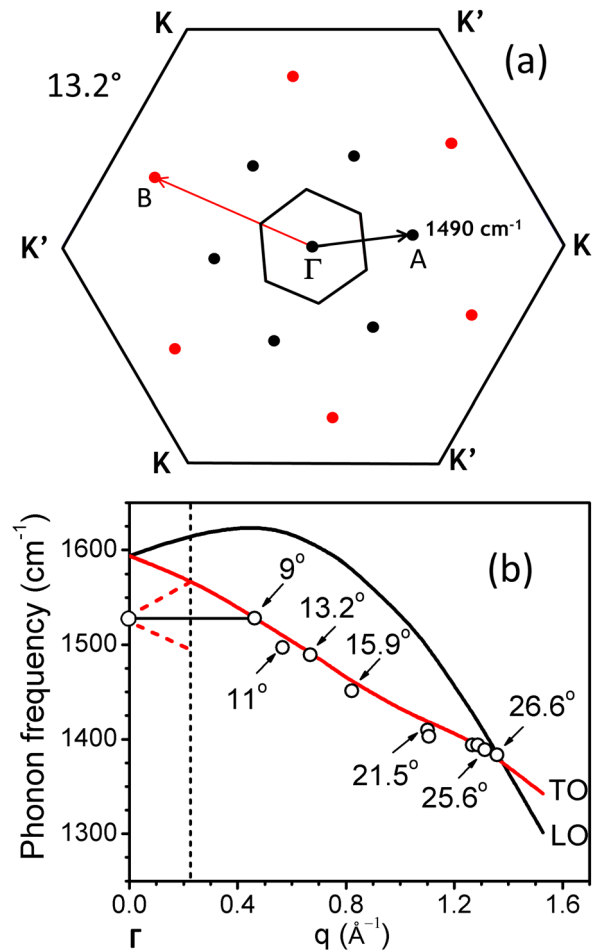


FIG. 5. Estimation of folded phonon frequency from transverse optical (TO) dispersion of single-layer graphene. (a) rBZ and reciprocal lattices of 13.2-degree twisted bilayer graphene in the BZ of single-layer graphene. The phonon marked by A can be excited by Raman with the exchange of crystal momentum Γ -A. (b) Calculated zone-folded phonon frequencies of TO and longitudinal mode (LO) as a function of reciprocal wave vector of bilayer superlattice or Moiré pattern. Circles are the observed folded TO phonons from Fig. 4(d).

studied bilayer graphene islands implies that tBLG synthesized by CVD are effective superlattices with a relatively strong interlayer coupling.

In conclusion, we synthesized isolated bilayer graphene hexagons and identified their superlattice structures using TEM, STM, and Raman scattering. We obtained G-line resonances and folded phonon spectra of tBLG with a wide range of rotation angles. Such Raman characterization provides a solid basis for further understanding and exploring rich physics and other unique properties of bilayer graphene. Single-layer graphene, a one-atom-thick two-dimensional lattice, thus provides us a different building block to engineer two-dimensional structures with tunable properties.

The work at Sandia National Laboratories was supported by the Office of Basic Energy Sciences, Division of Materials Sciences and Engineering of the U.S. DOE under Contract No. DE-AC04-94AL85000. S.-S.P., J.M.B., W.W., and S.R.X. acknowledge support from the Delta Electronics Foundation and UH CAM. J.M.B. acknowledges support from the National Science Foundation (Career Award ECCS-1240510 monitored by Anupama Kaul, DMR-0907336 monitored by Charles Ying) and the Robert A Welch Foundation (E-1728). V.G.H. work was supported by the State of Texas through the Texas Center for Superconductivity at the University of Houston. X.L. and Y.G. acknowledge support from Natural Science Foundation of China under Grant No. 11174347, and National Basic Research Program of China under Grant No. 2012CB933002.

¹J. M. B. Lopes dos Santos, N. M. R. Peres, and A. H. Castro Neto, *Phys. Rev. Lett.* **99**, 256802 (2007).

²S. Latil, V. Meunier, and L. Henrard, *Phys. Rev. B* **76**, 201402 (2007).

³A. H. MacDonald and R. Bistritzer, *Nature* **474**, 453 (2011).

⁴E. J. Mele, *Phys. Rev. B* **81**, 161405 (2010).

⁵A. Luican, G. H. Li, A. Reina, J. Kong, R. R. Nair, K. S. Novoselov, A. K. Geim, and E. Y. Andrei, *Phys. Rev. Lett.* **106**, 126802 (2011).

⁶K. Sato, R. Saito, C. X. Cong, T. Yu, and M. S. Dresselhaus, *Phys. Rev. B* **86**, 125414 (2012).

⁷J. Hicks, M. Sprinkle, K. Shepperd, F. Wang, A. Tejada, A. Taleb-Ibrahimi, F. Bertran, P. Le Fevre, W. A. de Heer, C. Berger, and E. H. Conrad, *Phys. Rev. B* **83**, 205403 (2011).

⁸S. Shallcross, S. Sharma, E. Kandelaki, and O. A. Pankratov, *Phys. Rev. B* **81**, 165105 (2010).

⁹A. Cocemasov, D. Nika, and A. Balandin, *Phys. Rev. B* **88**, 035428 (2013).

¹⁰K. Kim, S. Coh, L. Z. Tan, W. Regan, J. M. Yuk, E. Chatterjee, M. F. Crommie, M. L. Cohen, S. G. Louie, and A. Zettl, *Phys. Rev. Lett.* **108**, 246103 (2012).

¹¹J. Campos-Delgado, L. Cançado, C. Achete, A. Jorio, and J. Raskin, *Nano Res.* **6**, 269 (2013).

¹²Z. H. Ni, L. Liu, Y. Y. Wang, Z. Zheng, L. J. Li, T. Yu, and Z. X. Shen, *Phys. Rev. B* **80**, 125404 (2009).

¹³R. W. Havener, H. L. Zhuang, L. Brown, R. G. Hennig, and J. Park, *Nano Lett.* **12**, 3162 (2012).

¹⁴V. Carozo, C. M. Almeida, E. H. M. Ferreira, L. G. Cancado, C. A. Achete, and A. Jorio, *Nano Lett.* **11**, 4527 (2011).

¹⁵A. Righi, S. D. Costa, H. Chacham, C. Fantini, P. Venezuela, C. Magnuson, L. Colombo, W. S. Bacsa, R. S. Ruoff, and M. A. Pimenta, *Phys. Rev. B* **84**, 241409 (2011).

¹⁶S. Nie, W. Wu, S. R. Xing, Q. K. Yu, J. M. Bao, S. S. Pei, and K. F. McCarty, *New J. Phys.* **14**, 093028 (2012).

¹⁷Q. K. Yu, L. A. Jauregui, W. Wu, R. Colby, J. F. Tian, Z. H. Su, H. L. Cao, Z. H. Liu, D. Pandey, D. G. Wei, T. F. Chung, P. Peng, N. P. Guisinger, E. A. Stach, J. M. Bao, S. S. Pei, and Y. P. Chen, *Nature Mater.* **10**, 443 (2011).

¹⁸W. Wu, Z. H. Liu, L. A. Jauregui, Q. K. Yu, R. Pillai, H. L. Cao, J. M. Bao, Y. P. Chen, and S. S. Pei, *Sens. Actuators B* **150**, 296 (2010).

¹⁹See supplementary material at <http://dx.doi.org/10.1063/1.4821434> for graphene growth parameters, TEM, STM lattice Moiré patterns and phonon calculation.

²⁰G. H. Li, A. Luican, J. M. B. L. dos Santos, A. H. C. Neto, A. Reina, J. Kong, and E. Y. Andrei, *Nat. Phys.* **6**, 109 (2010).

²¹I. Vlasiouk, M. Regmi, P. F. Fulvio, S. Dai, P. Datskos, G. Eres, and S. Smirnov, *ACS Nano* **5**, 6069 (2011).

²²A. K. Gupta, Y. J. Tang, V. H. Crespi, and P. C. Eklund, *Phys. Rev. B* **82**, 241406 (2010).

²³I. Calizo, I. Bejenari, M. Rahman, G. Liu, and A. A. Balandin, *J. Appl. Phys.* **106**, 043509 (2009).

²⁴B. Jusserand and M. Cardona, in *Light Scattering in Solids V, Topics in Applied Physics*, edited by Gernot Guntherodt Manuel Cardona (Springer, Berlin, 1989), Vol. 66.

²⁵J. M. Bao, A. V. Bragas, J. K. Furdyna, and R. Merlin, *Phys. Rev. B* **71**, 045314 (2005).